Bimolecular DNA Triplexes: Duplex Extensions Show Implications for H-Form DNA Stability†

Andrew A. Mundt,*,‡ Gregory J. Crouch,§ and Bruce E. Eaton‡,§

Departments of Biochemistry and Biophysics and Chemistry, Washington State University, Pullman, Washington 99164-4660

Received March 20, 1997; Revised Manuscript Received August 14, 1997⊗

ABSTRACT: H-form DNA has recently been shown to be biologically relevant by its involvement in the process of homologous recombination [Kohwi, Y., and Panchenko, Y. (1993) *Genes Dev. 7*, 1766−1778]. A bimolecular DNA triple-stranded structure (triplex) is central to the formation of H-form DNA. Understanding the formation and factors governing the stability of such bimolecular triplexes is necessary to fully elucidate the structure/function relationship of H-form DNA. In this study, we extend known information on bimolecular triplexes by examining the effect of a variable CNC base triad (where N = A, C, T, or G) on a 10 base triad triplex that mimics the triplex motif in H-form DNA. We also examine the effect that a duplex extension of four base pairs has on triplex stability and selectivity for the base N. Results from thermal denaturation experiments indicate that the fully complementary triplex is more stable than its duplex counterpart ($\Delta T_m = 13$ °C) and is resistant to degradation by bovine spleen phosphodiesterase for at least 24 h at 10 °C. A single-base mismatch in the purine strand of the triplex structure is destabilizing ($\Delta T_m = \sim 20$ °C), and all structures containing a mismatch were readily degraded by bovine spleen phosphodiesterase. An extension of four duplex base pairs onto the triplex structure affects the stability of the DNA complex and may have implications relevant to H-form DNA.

Understanding the function of DNA structures in biology and the development of oligonucleotide-based biomolecular tools requires a clear understanding of the properties and limitations of such structures. Considerable work has been devoted to characterization of the canonical DNA duplex, but other structural forms of DNA have been less thoroughly studied. In recent years, interest in understanding triple-stranded DNA structures (triplexes) has increased because of the presence of triplexes in H-form DNA and sequence-specific recognition of duplex DNA by oligonucleotides resulting in triplex formation (*1*, *2*).

A DNA triplex is formed when a DNA strand occupies the major groove of a DNA double helix, associating with the purine-rich strand of a Watson−Crick duplex. The orientation of the third strand can be parallel or antiparallel to the purine duplex strand, and the association of the bases in the third strand with the purines in the duplex is through Hoogsteen or reverse-Hoogsteen hydrogen bonds, depending on the base triplets formed (*3*). Triplexes were initially found to form from three separate strands of oligonucleotides (*4*). To date, the termolecular form of the DNA triplex is the most studied triplex form, but other forms of triplexes do exist (see ref 5) for a comprehensive review). Intramolecular triplexes formed from a single strand of DNA are also known and have been examined (*6*). Bimolecular triplexes formed from two strands of DNA are also possible (*7*), but few examples have been reported despite their relevance as a model system for H-DNA *in vivo*.

Bimolecular triplexes are of particular interest because a bimolecular triplex is central to the formation of H-form DNA (*1*). H-form DNA is formed under superhelical stress from partially unwound duplex DNA where one strand folds back to interact with the remaining duplex, forming a triplex structure. Although H-form DNA was initially observed *in vitro*, it has been recently shown to exist *in vivo* (*8*). Experiments have also implicated H-form DNA as being involved in the process of homologous recombination (*9*). H-DNA can enhance recombination frequencies, and the stability of triplex structures may play a role in affecting this process. It is also reasonable to propose that the stability of H-DNA and concomitant triplex structures will affect DNA polymerization by blocking transcription. The role of H-form DNA in these biological processes remains to be fully understood.

Interest in triplex DNA is not limited to elucidating its biological role. The design and manipulation of nucleic acid structures is now viewed as a way of producing molecular tools with remarkable specificity and affinity (*10*, *11*). Dervan and Moser first showed that the triplex DNA motif could be used for sequence-specific strand cleavage (*12*). Other examples of using a triplex to act as a sequence-specific nuclease have expanded the possible DNA cleavage sites beyond known restriction enzymes (*12*). Triplexes have also been shown to block DNA and RNA polymerases at targeted sites, inhibiting replication or transcription processes (*13*−*20*). The ability of triplexes to block DNA polymerases is of interest in the development of anti-gene therapeutics (reviewed in ref *21*).

Developing triplex DNA as a molecular tool and understanding its biological role necessitates a knowledge of the thermodynamic stability and selectivity of triplex structures. Much of the information already determined is based on the termolecular form of triplexes (*22*−*26*). The first report on

† This work was supported by NeXstar Pharmaceuticals, Boulder, CO.

* To whom correspondence should be addressed. Current address: Bio-Logic, 1 rue de l'Europe, F-38640 Claix, France.

‡ Department of Biochemistry and Biophysics.

§ Department of Chemistry.

⊗ Abstract published in *Advance ACS Abstracts,* October 1, 1997.

S0006-2960(97)00658-2 CCC: $14.00

the relative stability of mismatches in termolecular triplexes at pH 5.6 showed some important differences in the thermal stability of triplet motifs (26). Biologically relevant bimolecular triplexes have been less studied. To extend this information, we examine the stability and selectivity of small bimolecular triplexes similar to that seen in H-form DNA. In addition, we examine the effect of extending the duplex region of a triplex on the stability and selectivity of the triplex.

EXPERIMENTAL PROCEDURES

Thermal Denaturation Studies. Thermal denaturation experiments used a Varian-Cary 2200 UV/VIS spectrophotometer equipped with thermostatable sample and reference bases, a Neslab EN-150 Flowthru cooler, and a Neslab EX-100 excal bath circulator equipped with an ETP-3 temperature programmer. All DNA oligomers were purchased from Operon Technologies Inc. and examined by HPLC for purity. Samples for thermal denaturation experiments contained a 1:1 ratio of each oligomer (~2.5 μM each unless otherwise noted). Also present was 50 mM Na_2HPO_4, 10 mM $MgCl_2$, 50 mM NaCl, and 2 mM EDTA at pH 7.0. All samples were annealed by heating them to 60 °C for 10 min and then allowing them to gradually cool to room temperature. Samples were added to a 1-cm path length 1.5-mL quartz cuvette and placed in the spectrophotometer set to dual-beam optical mode. A cuvette containing only buffer was used as the reference. The samples were cooled to starting temperatures at a rate of ~1.5 °C/min. The spectrophotometer was purged with dry N_2 at temperatures below 10 °C to protect against condensation. Thermal denaturation curves were obtained by recording the absorbance at 260 nm at 10-s intervals as the temperature was ramped at 1.0 °C/min (~200 data points/curve). Data was collected on a Varian DS-15 data station. The temperature was monitored in the blank and checked periodically in the sample cell using a portable digital thermometer. After the first thermal denaturation curve, samples were cooled in the spectrophotometer back to the starting temperatures, and the thermal denaturation process was repeated 2−4 times for each sample. Melting temperature (T_m) values were determined from the maximum of the first derivative of absorbance versus temperature curves. Reported T_m values are the average of all replicates for a given sample. All samples displayed sharp, apparently two-state transitions upon melting unless otherwise noted.

Thermodynamic Parameters. Free energies of duplexes and triplexes were determined from ΔH and ΔS values extracted from the thermal denaturation curves using the method of Petersheim and Turner (*27*). Free energies are listed wherever a good fit by the method was achieved. The fitting was limited by the quality of the lower temperature limit data in some cases.

Exonuclease Cleavage. Samples of proposed triplexes were prepared by mixing 50 pmol of each strand in ddH_2O. Each sample was then lyophilized and resuspended in 29 μL of 0.5 M ammonium acetate (pH 6.5). Samples were incubated at 60 °C for 10 min and allowed to cool over time to anneal them. The samples were then cooled to 10 °C at a rate of 1 °C/min in a Fisher Scientific Isotemp refrigerated circulator (Model 9500). Samples were then allowed to equilibrate at 10 °C for 15 min. One microliter (0.05 U) of phosphodiesterase II (bovine spleen phosphodiesterase; United States Biochemical) was added to each sample, and the reactions were incubated at 10 °C for 24 h. Reactions were stopped, and DNA was desalted using DuPont NENSORB-20 columns. The desalted DNA was lyophilized and then 5′-end labeled using T4 polynucleotide kinase and [γ-^{32}P]ATP. The labeling reaction was done at 55 °C for 24 h to maximize incorporation of ^{32}P. Each sample (~2 × 10^5 dpm) was lyophilized and resuspended in 5 μL of loading buffer (50:50, 40% sucrose:formamide). The samples were incubated at 60 °C for 10 min, and the reaction products were separated by electrophoresis on a denaturing 19% polyacrylamide gel alongside DNA size markers. DNA bands were visualized by autoradiography using Amersham Hyperfilm-MP.

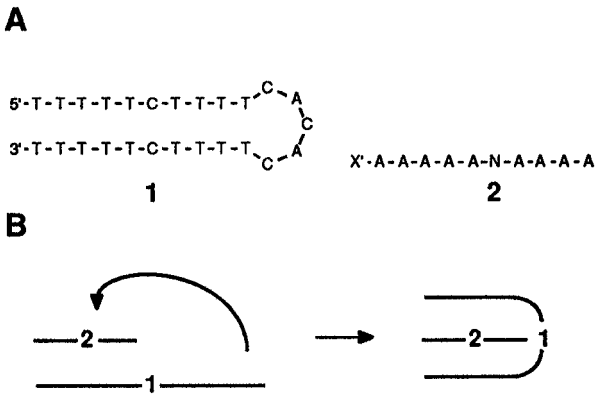

FIGURE 1: (A) Sequences of DNA used in this study to form bimolecular triplexes. X′ can be either 5′ or 3′ and N = A, G, C, or T. (B) Proposed formation of duplex and triplex structures from **1** and **2**.

RESULTS

Design of Bimolecular Triplexes. Oligonucleotide **1** (Figure 1A) was designed to contain a mirror repeat linked by a five nucleotide loop. One half of **1** can form a standard antiparallel duplex with single-stranded target containing sequence **2**. The other half of **1** is proposed to fold back and bind to the major groove of the **1·2** duplex, forming a triplex structure mimicking H-form DNA (Figure 1B) (*1*). The linking nucleotide loop was chosen to be five nucleotides in length since it has been demonstrated by Kool and Prakash that a five nucleotide loop is the desired length for triplex binding to single-stranded DNA (*28*). Sequence **2** was chosen for study because it has a minimal length for obtaining a stable duplex structure, and it is a simple example having sequence nonsymmetry. The nonsymmetry of sequence **2** allowed the formation of a duplex with the 3′- or 5′-half of **1** to be studied by altering the sequence direction of **2** (5′−3′ or 3′−5′).

Stability Studies. Thermal denaturation experiments were used to examine the stability and selectivity of bimolecular triplexes of the form indicated in Figure 1. Clearly, triplex formation is destablized by a mismatch at either of the Watson−Crick strands or the Hoogsteen strand. It was of interest to begin these investigations with mismatches only in the central DNA strand because it would have the potential to impact both the Watson−Crick and Hoogsteen interactions. Biologically, this could occur in H-DNA in the absence of effective DNA repair and would be expected to have the most dramatic impact on triplex stability. Other important biological roles for this type of triplex mismatch

Table 1: Structures, Melting Temperatures, and Thermodynamic Properties of **3**−**9**[a]

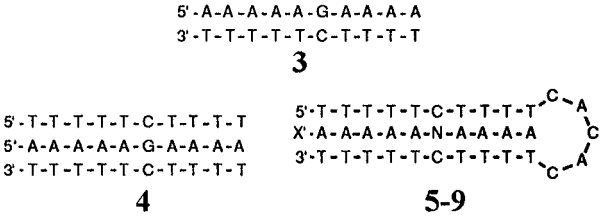

entry	X	N	T_m (°C)	ΔT_m[b] (°C)	$\Delta G°_{37}$ (kcal/mol)
3			22.4 ± 0.3	12.8	−4.71 ± 0.29
4			22	13	
5	5	G	35.2 ± 0.4		−7.57 ± 0.02
6	5	A	16.0 ± 0.7	19.2	
7	5	C	16.2 ± 0.3	19.0	
8	5	T	12.1 ± 0.7	23.1	
9	3	G	37.2 ± 0.2		−8.17 ± 0.12

[a] Melting temperatures were measured and thermodynamic properties calculated as described in Experimental Procedures. Values are listed as mean ±SD. [b] $\Delta T_m = T_m(\mathbf{5}) - T_m(\#)$.

could include differential regulation of gene expression by blocking transcription. In addition, it has recently been shown that triplex formation can lead to enhanced mutation rates and may be a source of genetic instability (*29*, *30*). Table 1 describes the series of complementary and singly-mismatched target strands incubated with **1** and lists the average T_m determined for each pairing from thermal denaturation experiments. Duplex **3** and the termolecular triplex **4** were also examined for comparison to the bimolecular triplexes. Melting experiments on the termolecular triplex **4** gave T_m values within experimental error of those observed for the corresponding duplex **3**. The hyperchromicities on melting of **3** and **4** were consistent with a two-state transition from duplex to single-stranded DNA for **3** and triplex to single-stranded DNA for **4**. Similar results have been reported previously for other termolecular triplexes melting at high ionic strength and low pH (pH = 5.8) (*31*). In contrast, triplex loop motif **5** gave a significant increase in T_m (ΔT_m = 12.8 °C) over that of duplex **3**, corresponding to a $\Delta\Delta G_{37}(\mathbf{5}-\mathbf{3}) = -2.87$ kcal/mol (*27*). The hyperchromicity on melting of **5** was 21%, consistent with a two-state transition. The apparent two-state nature of the melting of **5**−**9** indicates that these bimolecular triplexes show cooperative binding (*32*).

Due to the unusual stability of triplex **5**, the enthalpy and entropy of triplex **5** was examined in more detail. Table 2 shows the results of examining how the concentration of triplex **5** changes the temperature of thermal denaturation. ΔH, ΔS, and $\Delta G°$ values were determined from the denaturation curves by the method of Petersheim and Turner (*27*). The thermodynamic parameters were also determined by plotting $1/T_m$ versus ln C_T according to

$$1/T_m = (R/\Delta H°) \ln [C_T] + (\Delta S° - R \ln 4)/\Delta H°$$

where C_T is the concentration of each strand (*33*, *34*). The experimentally determined values for the binding energetics of **5** were in reasonable agreement between the two methods. It should be noted that the enthalpy and entropy values observed for **5** at pH 7 are similar to those previously reported for a comparable bimolecular triplex at pH = 5 (*35*).

Mismatch Studies. Thermal denaturation studies were also used to examine the selectivity of **1** for its target sequence. It is well known that the CGC motif is more stable at lower pH (∼5) when the N(3)-nitrogen of the cytidine in the third parallel strand is protonated allowing for tighter Hoogsteen binding (*36*, *37*). This suggests that the weakest base association in **5** would be the central CGC and that mismatches at this position would primarily decrease the binding energy by destabilizing the Watson−Crick portion of this triplet motif. This situation is analogous to the formation of H-form DNA in a duplex mismatch region where the mismatch is in the purine strand. Substitution of each of the three other bases for G (**6**−**8**, Table 1) in the central strand resulted in a dramatic drop in the T_m (∼20 °C). The difference in T_m between **5** and the mismatched triplexes (**6**−**8**, Table 1) is a measure of the selectivity of **1** for its target sequence. The ΔT_m values indicate that **1** can tolerate either a CAC or CCC triplet more than a CTC triplet. These results are similar to those seen for bimolecular triplexes formed from a circular single strand of DNA and a single strand target (*38*). The T_m data support the idea that the cooperative binding of the bimolecular triplexes studied allows for the sequence to be read twice even for a CGC triplet at pH = 7.

Target Sequence Orientation. The orientation of the target strand with respect to the loop region of **1** was examined by thermal denaturation. The sequence of the target strand in **5** was reversed in **9** so that the 5′-end of the target strand was facing the loop bases instead of the 3′-end. The T_m of **9** was slightly higher than the T_m of **5** (Table 1), indicating that either end of the target strand could be accommodated by the bases in the loop. A slight increase in the stability of H-form DNA and other bimolecular triplexes with the 5′-end facing the bridging loop bases has been reported previously by others (*39*). The origin of this difference in stability has yet to be explained in detail.

Exonuclease Studies. The thermal denaturation studies used to probe the triplexes proposed above only provide a macroscopic view of structure. The possibility existed that unusual motifs other than triplexes could be occurring. It was of interest to examine the proposed triplexes above and correlate the structures with the observed thermal denaturation data. The triplexes proposed in Table 3 were designed to take advantage of the phosphodiester cleavage properties of bovine spleen phosphodiesterase (BSP). BSP is an exonuclease that sequentially cleaves the phosphodiester backbone of single-stranded DNA in the 5′−3′ direction. Triplexes **10**−**13** are similar to **5**−**8** except that the central target strand has been extended by six bases in the 5′ direction beyond the triplex region. Triplexes with the 3′-end facing the loop bases were used in this study so that the Hoogsteen region of the triplex, if unbound, would be degraded by BSP, and the extended region of the target strand could be used as an internal standard to assess the activity of BSP. Thermal denaturation studies of **10** indicated no significant difference in T_m from that of **5**. All phosphodiesterase experiments were done in 0.5 M NH_4OAc, pH 6.5, to optimize enzyme activity. Thermal denaturation studies of **10** done in 0.5 M NH_4OAc, pH 6.5, indicated the T_m was not significantly different than that previously determined in phosphate buffer. Exonuclease experiments were performed on **10**−**13** (Table 3) as described in the Experimental Procedures. Figure 2 is of the denaturing 19% polyacrylamide gel showing the results of the experiment. The gel illustrates that **11**−**13** are degraded and only **10** appears to

Table 2: Melting Temperatures and Thermodynamic Properties for Concentration Series of **5**[a]

C_T (μM/strand)	T_m (°C)	ΔH (kcal/mol)	ΔS (e.u.)	$\Delta G°_{37}$ (kcal/mol)
1.2	34.7 ± 0.2	−100 ± 2	−297 ± 8	−8.28 ± 0.10
3.5	35.2 ± 0.4	−119 ± 9	−359 ± 29	−7.57 ± 0.02
39.3	39.2 ± 0.3	−111 ± 1	−334 ± 1	−7.36 ± 0.03
103	40.2 ± 0.1	−106 ± 1	−318 ± 6	−7.36 ± 0.05
average		−110 ± 5	−331 ± 16	−7.63 ± 0.22
from $1/T_m$ vs ln C_T		−144 ± 15	−438 ± 44	

[a] Melting temperatures were measured and thermodynamic properties calculated as described in Experimental Procedures. Values are listed as mean ±SD except for averages, which are listed as mean ±SE.

Table 3: Structures of **10**−**13**

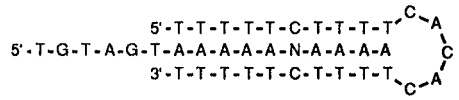

10-13

entry	Y
10	G
11	A
12	C
13	T

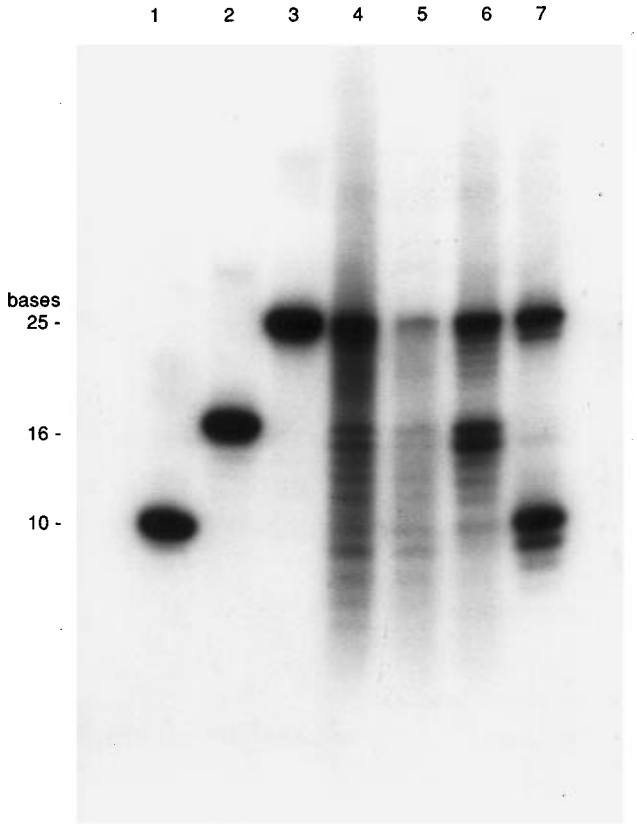

FIGURE 2: Autoradiogram of the 19% denaturing polyacrylamide gel obtained after reaction of oligonucleotide complexes **10**−**13** with bovine spleen phosphodiesterase for 24 h at 10 °C and subsequent labeling with T4 polynucleotide kinase and [γ-^{32}P]ATP. Lanes 1−3 are DNA size markers of 10, 16, and 25 bases, respectively. Lanes 4−7: lane 4, **11**; lane 5, **12**; lane 6, **13**; and lane 7, **10**.

be resistant to cleavage by BSP. These results are consistent with the thermal denaturation data indicating the instability of a bimolecular triplex with a mismatch.

Duplex Region Extensions. In H-form DNA, single-stranded and duplex DNA extend beyond the triplex region. Interactions between the loop region of the triplex and the single-stranded extension affects the stability of H-form DNA and other bimolecular triplexes (*28*, *40*, *41*). The effect of duplex DNA extending beyond the triplex region on bimolecular triplex formation has previously not been examined.

Table 4: Structures and Melting Temperatures of **14**−**18**[a]

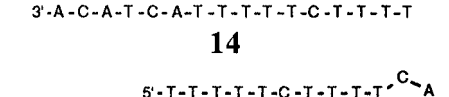

14

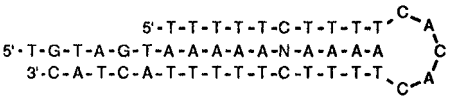

15-18

entry	Y	T_m (°C)	entry	Y	T_m (°C)
14		45.3 ± 0.1	**17**	C	28.3 ± 0.3
15	G	43.9 ± 0.7	**18**	T	32.6 ± 0.7
16	A	31.6 ± 0.3			

[a] Melting temperatures were measured as described in Experimental Procedures. Values are listed as mean ±SD.

The effect of a duplex extension on triplex formation was examined by thermal denaturation studies. The triplexes in Table 4 were designed to have identical triplex regions to triplexes in Tables 2 and 3. It was expected that the duplex region would have little or no effect on the formation and stability of a bimolecular triplex, based on the formation of a triplex in H-form DNA. Table 4 and Figure 3 indicate that the duplex extension had a significant effect upon the stability of the triplex studied. The fully complementary triplex **15** showed little difference in T_m from that of duplex **14** although the thermal denaturation curve of **15** indicated only a single transition and the hyperchromicity was consistent with two-state behavior (Figure 3). Figure 3 indicates that the introduction of a mismatch into the triplex results in non-two-state melting behavior. Both the thermal denaturation traces of **16**−**18** and their respective first derivatives indicate the presence of two transitions. It is assumed that the lower of the two transitions corresponds to the melting of the Hoogsteen strand and that the upper transition corresponds to the melting of the remaining duplex. The T_m values for the upper transition are listed in Table 4. The T_m values for the lower transitions of the mismatched triplexes are not listed as the lower transition could not be measured accurately. Exonuclease experiments performed on **15** confirmed the stability of **15** indicated by the thermal denaturation experiments (data not shown). The exonuclease experiment results showed some degradation of the Hoogsteen portion of **15**, resulting in a faint band at 30 bases, the intact strand, and a distribution of bands ∼12−16 bases in length.

The duplex extension also altered the order of selectivity for the variable base N in **15**−**18** as compared with selectivity

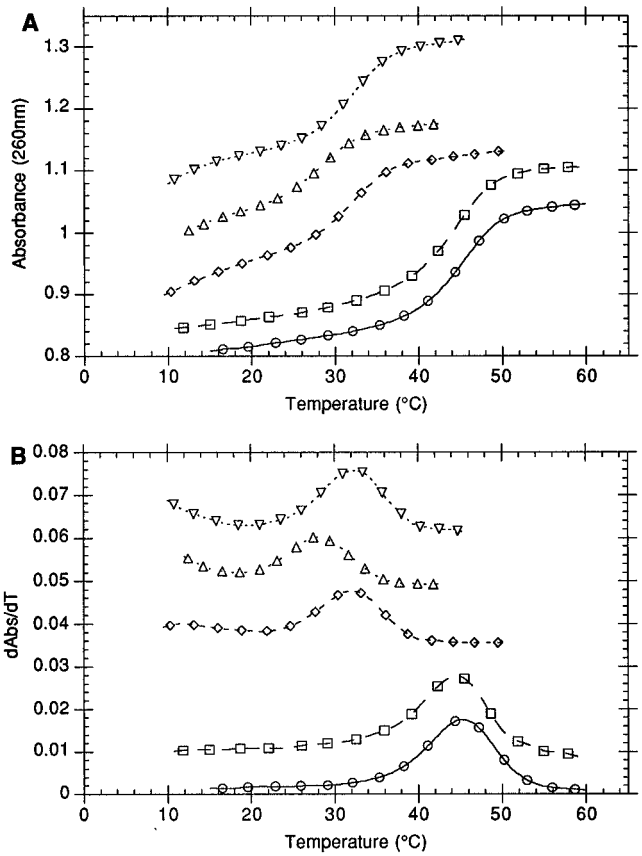

FIGURE 3: (A) Thermal denaturation traces of **14**−**18**. (B) First derivative traces of thermal denaturation traces for **14**−**18**. The traces are offset for clarity, and the conditions are described in Experimental Procedures. Symbol definitions: (○) **14**, (□) **15**, (◇) **16**, (△) **17**, and (▽) **18**.

for N seen in **5**−**8**. Table 1 indicates the selectivity for N in **5**−**8** is G > C = A > T. The addition of four base pairs in **15**−**18** changes the selectivity for N to G > T ≥ A > C (Table 4). The selectivity shown by **15**−**18** is the same as that exhibited by a series of simple duplexes with a CN base pair (*38*). The similarity in mismatch preference between **15**−**18** and duplex DNA could be interpreted to indicate that the combination of the duplex extension and a mismatch present in the triplex region may completely destabilize triplex formation.

DISCUSSION

Effects of Mismatches in Bimolecular Triplexes. Table 1 displays the effects of a CNC triplet mismatch in the bimolecular triplex studied. This is presumably similar to the formation of H-form DNA in a region of DNA containing a single transition or transversion mutation in the purine strand of the triplex. The results presented here indicate that a mutation is extremely costly ($\Delta T_m = \sim 20$ °C) in terms of stability. This is significant since H-form DNA has been shown to form *in vivo* and may be involved in the process of recombination (*9*). The cost of mutations studied here are in agreement with mismatch studies done on similar bimolecular triplexes (*38*). Taken together, the T_m values for all bimolecular triplexes studied to date indicate that the cost of mutations in the target strand of a bimolecular triplex is greater than a mismatch in only the Hoogsteen or only the Watson−Crick region of the triplex (*38*, *42*). This is expected since mutations in the target strand can perturb both Watson−Crick and Hoogsteen interactions. It has been reported that H-form DNA can form even with the presence of a mutation that disrupts the Hoogsteen or Watson−Crick region of the triplex, although the mismatch significantly destabilizes the structure (*2*, *43*). It has yet to be determined whether H-form DNA can form in the presence of a transition or transversion mutation in the target strand.

Effects of Duplex Extension on Triplex Stability. The results in Table 4 indicate that the presence of an extended duplex region abolishes the energetic enhancement provided by the formation of a bimolecular triplex. The similarity of T_m values between the duplex **14** and the triplex **15** is in contrast to the ΔT_m of 13 °C seen between duplex **3** and triplex **5** that favors the formation of a bimolecular triplex. In addition, exonuclease experiments on **5** and **15** indicate that **15** is more susceptible to attack by BSP than **5**. The comparable stability of a duplex versus a duplex/triplex chimeric structure has also been reported by others, but comparison with a similar triplex-only structure was not examined (*7*).

The reason for the lack of enhanced stability in a duplex/triplex chimeric structure is not entirely clear. The difference between **5** and **15** of only an additional four base pairs in the duplex region suggests that the additional duplex base pairs restricted the available conformational states so that previously accessible geometries of the duplex region were made inaccessible. As evidenced by the limited number of commonly seen stable forms of duplex DNA, it is reasonable to assume that there are only certain regions of conformational space where triplexes are stable as well and where bimolecular triplexes are more stable than structurally similar duplexes.

Table 4 also indicates that the presence of a duplex extension alters the order of stability of structures containing a CNC mismatch (**15**−**18**) as compared with similar structures without a duplex extension (**5**−**8**, Table 1). This effect may be due to the restriction of conformational states for triplex or duplex structures and may reflect a competition that diminishes favorable interactions depending on the length of duplex and triplex for an H-form DNA segment. The observation that the order of stability of **15**−**18** parallels that for a similar series of duplexes indicates that the combined effect of the duplex extension and the introduction of a mismatch into the triplex region may completely destabilize triplex formation (*38*). Alternatively, thermal denaturation experiments on termolecular triplexes that contained duplex extensions have shown that triplet motifs other than the cononical forms could show significant stability. For example, at pH 5.6 (1 M NaCl) CGC in the middle of a 13 nucleotide triplex was shown to be of similar stability to TGC, where TG was the mismatched Watson−Crick pair. Thus, the interplay between juxtaposed duplex and triplex sequences remains to be fully understood.

The results presented here do not reveal if the effect of the duplex extension on triplex stability is due to the length of the duplex region or if it is a sequence effect. Clearly both the length and the sequence may play a role in the case of biologically relevant H-form DNA, where an extended duplex region is always present. Although the idea of a sequence effect brings to mind the possibility of triplex enhancer and repressor sequences, further research needs to be done before conclusions can be made.

CONCLUSIONS

The results presented here show that internal mismatches of the form CNC, where N is any base other than G, significantly affect the stability of the bimolecular triplex studied. A single mismatch destabilizes the triplex examined so that it becomes susceptible to degradation by BSP. The fully complementary bimolecular triplex is resistant to BSP digestion for at least 24 h. The results also indicate that a duplex extension of four base pairs eliminates the enhanced stability of the triplex over its duplex counterpart. The addition of four duplex base pairs was also shown to alter the order of stability of studied triplexes with a CNC mismatch. Finally, there appears to be a delicate balance for bimolecular triplex formation and stability that may be important in the formation of H-form DNA and its role in regulating biological processes.

ACKNOWLEDGMENT

We thank Dr. Dom Zichi of NeXstar Pharmaceuticals for his help in extracting thermodynamic parameters from thermal denaturation curves.

REFERENCES

1. Lyamichev, V. I., Mirkin, S. M., and Frank-Kamenetskii, M. D. (1986) *J. Biomol. Struct. Dyn. 3*, 667−669.
2. Mirkin, S. M., Lyamichev, V. I., Drushlyak, K. N., Dobrynin, V. N., Filippov, S. A., and Frank-Kamenetskii, M. D. (1987) *Nature 330*, 495−497.
3. Hoogsteen, K. (1959) *Acta Crystallogr. 12*, 822−823.
4. Felsenfeld, G., Davies, D. R., and Rich, A. (1957) *J. Am. Chem. Soc. 79*, 2023−2024.
5. Frank-Kamenetskii, M. D., and Mirkin, S. M. (1995) *Annu. Rev. Biochem. 64*, 65−95.
6. Häner, R., and Dervan, P. B. (1990) *Biochemistry 29*, 9761−9765.
7. Noll, D. M., O'Rear, J. L., Cushman, C. D., and Miller, P. S. (1994) *Nucelosides Nucleotides 13*, 997−1005.
8. Karlovsky, P., Pecinka, P., Vojtiskova, M., Makaturova, E., and Palecek, E. (1990) *FEBS Lett. 274*, 39−42.
9. Kohwi, Y., and Panchenko, Y. (1993) *Genes Dev. 7*, 1766−1778.
10. Gold, L., Tuerk, C., Allen, P., Binkley, J., Brown, D., Green, L., MacDougal, S., Schneider, D., Tasset, D., and Eddy, S. (1993) in *The RNA World* (Gespeland, A., & Atkins, J., Eds.) pp 497−509, Cold Springs Harbor Laboratory Press, Plainview, NY.
11. Eaton, B. E., Gold, L., and Zichi, D. A. (1995) *Chem. Biol. 2*, 633−638.
12. Moser, H. E., and Dervan, P. B. (1987) *Science 238*, 645−650.
13. Mergny, J. L., Duval-Valentin, G., Nguyen, C. H., Perrouault, L., Faucon, B., Rougée, M., Montenay-Garestier, T., Bisagni, E., and Hélène, C. (1992) *Science 256*, 1681−1684.
14. Baran, N., Lapidot, A., and Manor, H. (1991) *Proc. Natl. Acad. Sci. U.S.A. 88*, 507−511.
15. Duval-Valentin, G., Thuong, N. T., and Hélène, C. (1992) *Proc. Natl. Acad. Sci. U.S.A. 89*, 504−508.
16. Guieysse, A. L., Praseuth, D., Francois, J. C., and Hélène, C. (1995) *Biochem. Biophys. Res. Commun. 217*, 186−194.
17. Hacia, J. G., Dervan, P. B., and Wold, B. J. (1994) *Biochemistry 33*, 6192−6200.
18. Lapidot, A., Baran, N., and Manor, H. (1989) *Nucleic Acids Res. 17*, 883−900.
19. Samadashwily, G. M., Dayn, A., and Mirkin, S. M. (1993) *EMBO J. 12*, 4975−4983.
20. Samadashwily, G. M., and Mirkin, S. M. (1994) *Gene 149*, 127−136.
21. Hélène, C. (1991) *Anticancer Drug Des. 6*, 569−584.
22. Beal, P. A., and Dervan, P. B. (1992) *Nucleic Acids Res. 20*, 2773−2776.
23. Mergny, J. L., Sun, J. S., Rougée, M., Montenay-Garestier, T., Barcelo, F., Chomilier, J., and Hélène, C. (1991) *Biochemistry 30*, 9791−9798.
24. Plum, G. E., Park, Y. W., Singleton, S. F., Dervan, P. B., and Breslauer, K. J. (1990) *Proc. Natl. Acad. Sci. U.S.A. 87*, 9436−9440.
25. Plum, G. E., Pilch, D. S., Singleton, S. F., and Breslauer, K. J. (1995) *Annu. Rev. Biophys. Biomol. Struct. 24*, 319−350.
26. Sun, J. S., Mergny, J. L., Lavery, R., Montenay-Garestier, T., and Hélène, C. (1991) *J. Biomol. Struct. Dyn. 9*, 411−424.
27. Petersheim, M., and Turner, D. H. (1983) *Biochemistry 22*, 256−263.
28. Prakash, G., and Kool, E. T. (1992) *J. Am. Chem. Soc. 114*, 3523−3527.
29. Wang, G., Seidman, M., and Glazer, M. (1996) *Science 271*, 802−805.
30. Brereton, H. M., Firgaira, F. A., and Turner, D. R. (1993) *Nucleic Acids Res. 21*, 2563−2569.
31. Rougée, M., Faucon, B., Mergny, J. L., Barcelo, F., Giovannangeli, C., Garestier, T., and Hélène, C. (1992) *Biochemistry 31*, 9269−9278.
32. Prakash, G., and Kool, E. T. (1991) *J. Chem. Soc. Chem. Commun.* 1161−1163.
33. Marky, L. A., and Breslauer, K. J. (1987) *Biopolymers 26*, 1601−1620.
34. Martin, F. H., Uhlenbeck, O. C., and Doty, P. (1971) *J. Mol. Biol. 57*, 201−215.
35. Xodo, L. E., Manzini, G., and Quadrifoglio, F. (1990) *Nucleic Acids Res. 18*, 3557−3564.
36. Rajagopal, P., and Feigon, J. (1989) *Nature 339*, 637−640.
37. de los Santos, C., Rosen, M., and Patel, D. (1989) *Biochemistry 28*, 7282−7289.
38. Kool, E. T. (1991) *J. Am. Chem. Soc. 113*, 6265−6266.
39. Shimizu, M., Hanvey, J. C., and Wells, R. D. (1989) *J. Biol. Chem. 264*, 5944−5949.
40. Shimizu, M., Kubo, K., Matsumoto, U., and Shindo, H. (1994) *J. Mol. Biol. 235*, 185−197.
41. Wang, S., Booher, M. A., and Kool, E. T. (1994) *Biochemistry 33*, 4639−4644.
42. Wang, S., Friedman, A. E., and Kool, E. T. (1995) *Biochemistry 34*, 9774−9784.
43. Belotserkovskii, B. P., Veselkov, A. G., Filippov, S. A., Dobrynin, V. N., Mirkin, S. M., and Frank-Kamenetskii, M. D. (1990) *Nucleic Acids Res. 18*, 8821−8824.

BI970658Y